Ultrasonics Sonochemistry 130 (2026) 107905

Contents lists available at ScienceDirect

Ultrasonics Sonochemistry

journal homepage: www.elsevier.com/locate/ultson

Optimal ultrasound enhances T. *reesei* cellulases secretion for high biomass enzymatic saccharification by hyphal fragmentation

Hao Peng [a,b,c,1], Jingyuan Liu [a,b,1], Jiale Liu [a], Xueyu Wang [a], Hailang Wang [a,c], Huan Ma [c], Yansong Fu [c], Dan Sun [a], Yanting Wang [a], Chunxiang Fu [b], Liangcai Peng [a,c], Peng Liu [a,*]

[a] *Key Laboratory of Fermentation Engineering (Ministry of Education), National "111" Center for Cellular Regulation & Molecular Pharmaceutics, Cooperative Innovation Center of Industrial Fermentation (Ministry of Education & Hubei Province), Hubei Key Laboratory of Industrial Microbiology, School of Life & Health Sciences, Hubei University of Technology, Wuhan 430068, China*

[b] *Shandong Provincial Key Laboratory of Energy Genetics, CAS Key Laboratory of Biofuels, Qingdao Institute of Bioenergy & Bioprocess Technology, Chinese Academy of Sciences, Shandong Energy Institute, Qingdao New Energy Shandong Laboratory, Qingdao 266101, China*

[c] *College of Plant Science & Technology, Huazhong Agricultural University, Wuhan 430070, China*

ARTICLE INFO

Keywords:
Ultrasound
Sugarcane bagasse
Fungal incubation
Cellulases
Xylanases
Bioenergy crops

ABSTRACT

Although ultrasound technology has been broadly employed in diverse fields, its direct application during fungal incubation for production of lignocellulose-degrading enzymes is not implemented. Using sugarcane bagasse together with sugarcane juice, this study optimized *T. reesei* incubation condition for secretion of mixed-cellulases at high activities. The optimal ultrasound treatment was then explored to improve enzyme production during *T. reesei* incubation with the bagasse substrate for secretions of three major types of cellulases and xylanases. As a comparison, the secreted CBHI, EGII, β-glucosidase and xylanase activities were respectively increased by 48%, 10%, 147% and 74%, whereas the FPA was raised by 54% relative to the control (without ultrasound). Furthermore, those secreted enzymes were employed for biomass enzymatic saccharification in three representative bioenergy crops after mild alkali pretreatments, with raised hexose yields by 50%-64% and total sugar yields by 34%-43%. Notably, we observed the hyphal fragmentation at well distribution and the digested lignocelluloses at high homogeneity during a long-term *T. reesei* incubation after optimal ultrasound treatment. Meanwhile, untargeted metabolomic profiling revealed a distinctively altered metabolic remodeling in both fungal-secreted enzymes and all remaining fungal-lignocellulose residues under optimal ultrasound treatment. Based on all major findings achieved, a model is finally proposed about the distinct roles of optimal ultrasound treatment for improving *T. reesei* secretion of cellulases and xylanases at high-yield and high-activity by facilitating *T. reesei* interaction with bagasse substrate. Therefore, this study has demonstrated an advanced ultrasound technology to upgrade enzymes production from fungal-lignocellulose incubation for enhancing biomass enzymatic saccharification in bioenergy crops.

1. Introduction

Plant photosynthesis produces the most abundant lignocellulosic substances that can be converted into biofuels and biochemicals on the earth [1,2]. However, plant cell walls are naturally recalcitrant to biomass enzymatic saccharification, leading to costly lignocellulose conversion [3,4]. As a highly-efficient C4 plant, sugarcane is widely cultivated for sugar production, resulting in large amounts of lignocellulose-derived bagasse residues [5,6]. The sugarcane bagasse is of relatively low crystalline index (CrI) and degree of polymerization (DP) of cellulose microfibrils accountable for high biomass enzymatic saccharification [7–9]. Therefore, sugarcane bagasse is not only used for efficient bioethanol conversion, but is also considered an effective substrate for inducing fungal secretion of lignocellulose-degrading enzymes [10–12].

Because biomass enzymatic saccharification is a crucial step for cost-effective lignocellulose conversion, attempts have been made to produce high-yield lignocellulose-degrading enzymes with high-activity [13,14].

* Correspondence author.
E-mail address: liupeng@hbut.edu.cn (P. Liu).
URL: http://bbrc.hbut.edu.cn (P. Liu).
[1] The authors contributed equally.

https://doi.org/10.1016/j.ultsonch.2026.107905
Received 24 October 2025; Received in revised form 22 May 2026; Accepted 22 May 2026
Available online 24 May 2026

Over the past years, microorganisms have been cultured with different inducing carbon sources to secrete lignocellulose-degrading enzyme complexes, including four major types of enzymes: exoglucanases (CBHs), endoglucanase (EGs), β-glucosidases (BGs), and xylanases [15]. As a common filamentous fungus, *T. reesei* is used to produce high-activity CBHs and EGs [16,17]. Furthermore, as cellulose nanofibrils assembly determines the breakpoints for initiating and completing lignocellulose enzymatic hydrolysis, the length-reduced cellulose nanofibers have been incubated with fungal strains to secrete mixed-cellulases at high activities [18–20]. Nevertheless, due to the complex structures of diverse lignocellulose substrates, novel technology is required for optimal production of mixed-cellulases, enabling efficient enzymatic saccharification of biomass in different types of bioenergy crops [21].

As a sustainable technology, ultrasound treatment is increasingly applied for biomass pretreatment and enzymatic hydrolysis, due to its multiple advantages such as short-time operation, high-energy activation, and non-chemical loading [22,23]. Specifically, ultrasound treatment is effective for the partial extraction of hemicellulose and lignin, facilitating cellulase access and loading for lignocellulose hydrolysis [9,24]. Nevertheless, despite of ultrasound application in lignocellulose processes, a knowledge gap remains regarding its direct role in fungal incubation for high-yield and high-activity cellulases secretion.

By employing two sugarcane bagasse substrates (ROC22 and F134) responsible for distinct lignocellulose recalcitrance and cellulose nanofibrils assembly [3,7], this study detected higher-activity mixed-cellulases from F134 induction with *T. reesei in vitro* (Fig. S1). Notably, this work performed optimal ultrasound treatment during F134 incubation with two fungi strains, and examined distinctively enhanced activities of the secreted cellulases and xylanases. By employing the fungi-secreted enzymes solutions, we examined the remarkable enhancement of biomass enzymatic saccharification in three representative bioenergy crops (rice, eucalyptus, and fern). Based on these major findings, this study developed a hypothetical model that demonstrates ultrasound treatment's role in favoring distinct mixed-cellulases production for enhancing biomass enzymatic saccharification, providing a novel strategy for optimal cellulases production under an environmentally friendly process.

2. Materials and methods

2.1. Collection of biomass samples and enzymes

Biomass of two sugarcane cultivars (ROC22, F134) were harvested from the research fields located at Huazhong Agricultural University in Wuhan, China. The juice extracted from sugarcane stalk was obtained by pressing, and the bagasse was dehydrated at approximately 50–60 °C before being milled into powders using a 40-mesh screen. The extraction of soluble sugars was carried out using ddH_2O from the bagasse powders and the residual materials were placed in a desiccated container. Biomass samples of fern, eucalyptus and rice were obtained from the same research fields as sugarcane, dehydrated at 50–60 °C and pulverized into biomass powders. Four enzymes (endoglucanases, exoglucanases, β-glucosidases and xylanases) and commercial mixed-enzymes (HSB) were acquired from Megazyme and Imperial Jade Biotechnology Company, respectively.

2.2. Determination of wall polymers and its features

The wall polymers extraction and detection methods of sugarcane bagasse (ROC22, F134) were conducted as described [12]. Cellulose was measured by anthrone/H_2SO_4 method in the two samples. For arabinose (Ara) and xylose (Xyl) assay of total hemicellulose, GC–MS (Shimadzu GCMS-QP2010Plus) running was conducted [21]. Total lignin content was detected through two-step acid hydrolysis [25]. The monomers of lignin (H, S, G) were measured by HPLC [26]. For feature detection, the accessibility of cellulose was measured by Congo red [7]. Viscosity method with minor changes was carried out to measure the degree of polymerization (DP) of cellulose [27]. X-ray diffraction analysis was applied to measure the crystalline index (CrI) of cellulose of sugarcane bagasse [28].

2.3. T. reesei strain cultivation with sugarcane juice

The 0.6 g sugarcane bagasse (ROC22, F134) with 0%, 5%, 10%, 20%, 40% (soluble sugars % DM) dosage of sugarcane juice was utilized as the carbon source to co-cultivate with the *T. reesei* (Rut-C30, CICC40348). *T. reesei* was cultured on potato dextrose agar at 28–30 °C for a period of 7 days, and the conidia were obtained with double-distilled water and quantified with a haemocytometer. It was set at 6×10^6 spores every milliliter and 0.5 mL of solution was then co-cultivated with carbon source for 7 days at the temperature of 30 °C. The Mandels-Andreotti medium was performed and the pH value was ensured at 4.8 [18].

2.4. Ultrasound treatment for T. reesei strain incubation

T. reesei was co-cultivated with 0.6 g F134 sugarcane bagasse and optimal sugarcane juice (20% soluble sugars) as inducing substrates in 30 mL liquid culture under intermittent ultrasound treatments to induce cellulases production by using an ultrasonic processor (SB-3200DTD, Ningbo Scientz Biotechnology Co., Ltd, China). The key operating parameters of ultrasonic processor were as follows: frequency = 40 kHz; maximum rated ultrasonic power = 180 W; capacity = 6 L (internal dimensions: 300 × 155 × 150 mm). About 30 mL culture in a 100 mL Erlenmeyer flask was placed in the ultrasonic processor containing 1 L of ddH_2O (initial temperature 28 °C). The ddH_2O level covered the liquid culture inside the flask to an immersion depth of approximately 20 mm. For this study, the ultrasonic power output was set to 40%, 60% and 80% (72, 108, 144 W power) of the maximum for 1, 2, 4 min operation, respectively. As summarized in Table S1, three ultrasound schedules were tested during the 7-day *T. reesei* incubation: one-time treatment, three-time treatment and six-time treatment. The nominal input energy for each ultrasound treatment was estimated using the following equation: nominal input energy (J) = rated output power (W) × treatment time (s) × treatment repetition. The calorimetric measurements were performed to estimate the actual acoustic power delivered to the sample under the sonication configuration by using 30 mL deionized water in a 100 mL Erlenmeyer flask under the same nominal settings, immersion depth and configuration as applied in the cultivation experiments. The temperature rise of the sample was recorded at 0, 40, 80 and 120 s under nominal settings of 72, 108 and 144 W, respectively. The acoustic power was calculated according to $P = mC_p(dT/dt)$, where m is the sample mass and C_p is the specific heat capacity of water. The detailed temperature-rise curves and derived calorimetric parameters were shown in Fig. S2 and Table S2. After incubation, the solutions were then centrifuged for 5–10 min to obtain crude enzymes. Control experiment was meanwhile conducted without ultrasound treatment. Only fungi ultrasound was conducted for one time of optimal ultrasound treatment with *T. reesei* before incubation with sugarcane bagasse substrate. Only substrate ultrasound was completed for one time of optimal ultrasound treatment with bagasse substrate before incubated with *T. reesei* strain.

2.5. Filter paper activity (FPA) detection and total protein content

FPA and total protein content were respectively measured as described with minor changes [19,29]. A mixture of enzymes and buffer (1:3) was applied to Whatman filter paper. The mixed solution was shaken for 1 h at approximately 50 °C and the reaction was terminated by the addition of DNS and the boiling water for a duration of 10 min. Total protein content secreted by *T. reesei* was estimated by Coomassie Brilliant Blue G250 [18,30]. SDS-PAGE was performed to separate proteins using stain-free precast gels [31]. All assays were conducted at

independent triplicate.

2.6. Endoglucanases, exoglucanases, β-glucosidases and xylanases assay in vitro

The activities assays of four enzymes were conducted in accordance with previously established protocols using CMC-Na, pNPC, salicin and beechwood xylan [18]. Approximately 500 μL of crude enzyme and 1 mL of CMC-Na were performed to estimate endoglucanases activity at 50 °C for a duration of 30 min. Other three enzymes assays were determined under similar conditions by using pNPC, salicin and xylan solution, respectively [19]. Dinitrosalicylic acid method (DNS) was used to measure reducing sugars released except exoglucanases. The reaction was terminated by DNS and the absorbance was recorded at wavelength of 540 nm. For *exo*-glucanases assay, 0.75 mL of a solution containing 10% Na_2CO_3 was performed to terminate the reaction and the absorbance was measured at wavelength of 420 nm. All experiments were conducted under independent triplicate.

2.7. Enzymes supernatant characterization

The anthrone/H_2SO_4 method was employed to assay hexoses and the ferric chloride/HCl method was utilized for the determination of pentoses of the supernatants from the 3rd, 5th, 7th day during 7 days *T. reesei* strain incubation with F134 sugarcane bagasse and sugarcane juice (20% soluble sugars) under optimal ultrasound treatment [32,33]. Total protein contents of the enzymes on the 3rd, 5th, 7th day were detected as described above. The interfacial tension of supernatants on the 7th day were tested by a surface/interface tensiometer (K100, America) at 25 °C. Briefly, the crude enzymes were placed in a beaker and the test began after the plate was approached to the liquid level. The plate was burned for 3–5 min after the measurement was accomplished.

2.8. Lignocellulose characterization

The crystalline index (CrI) of lignocellulose residues after *T. reesei* incubation was detected by X-ray diffraction by scanning from 5° to 45° to acquire diffraction data, and CrI value was determined based on the peaks around 22.5° and 18° [28]. Fourier transform infrared (FT-IR) was also employed to characterize the lignocellulose residues [31].

2.9. Observation of T. reesei and sugarcane bagasse images

Fluorescence microscopy (Yongxin NE910, China) was applied to observe *T. reesei* incubation with F134 sugarcane bagasse co-supplied with 20% sugarcane juice under the optimal ultrasound treatments through Image View software. The *T. reesei* strain was stained with trypan blue and the sugarcane bagasse substrate was stained with Calcofluor for microscopic views.

2.10. Proteomics analysis

Lignocellulose-degradation enzymes secreted by *T. reesei* under optimal ultrasound treatment with 20% sugarcane juice were detected by LC-MS/MS (Jingjie PTM BioLab Co., Ltd., Hangzhou, China; Orbitrap Elite LC-MS/MS, Thermo, USA) as described before [18,19]. The peptides were analyzed utilizing NSI source followed by MS/MS (Tandem Mass Spectrometry). The electrospray voltage was set at 2.0 kV with a *m/z* scan range of 350–1600, and peptides were measured with the Orbitrap at 30,000 resolution. Peptides were subsequently selected using NCE setting as 35 and the fragments were analyzed with the Orbitrap at 17,500 resolution. A data-dependent procedure was employed alternating between one MS scan followed by 20 MS/MS scans with a dynamic exclusion time of 15.0 s.

2.11. Biomass enzymatic saccharification

Three lignocellulose samples (fern, rice, eucalyptus) were pretreated with 0.5% NaOH (w/v) solution at 50 °C for 2 h under shaking at 150 rpm. The remaining pellet after centrifugation was incubated with enzymes (cellulases of 10 FPU/g) solution produced by *T. reesei* at a temperature of 50 °C with a shaking speed of 150 rpm for 48 h [13,34]. Commercial enzymes of HSB (cellulases of 10 FPU/g) were meanwhile employed for biomass enzymatic saccharification. After centrifugation, the supernatant was collected to determine hexoses, pentoses and total sugars yields. All experiments were accomplished under independent triplicate.

2.12. Ergosterol estimation as an indirect fungal biomass proxy

After 7-day incubations under the optimal ultrasound treatment and the control (without ultrasound), the fungal-lignocellulosic residues were collected and freeze-dried. Approximately 0.1 g of each dried sample was well mixed with 4 mL of 25% KOH-methanol solution and incubated at 80 °C for 30 min for saponification. After cooling to room temperature, 2 mL deionized water and 4 mL hexane were added and vortexed for 2 min. The upper organic phase was collected, and the extraction was repeated once with an additional 4 mL hexane. The combined hexane extracts were evaporated to dryness and re-dissolved in 1 mL absolute ethanol. Ergosterol was then quantified by a UV-based assay at 282 nm using an ergosterol standard curve and expressed as μg/g dry weight. The ergosterol level was used as an indirect proxy for fungal biomass.

2.13. Untargeted metabolomic analysis

Enzymes and lignocellulose residues were collected after 7-day *T. reesei* incubation under the optimal ultrasound treatment and control (without ultrasound) condition. Metabolites were profiled using a Waters ACQUITY I-Class PLUS UPLC system coupled with a Xevo G2-XS QTOF mass spectrometer (Waters, USA). Separation was accomplished on an ACQUITY UPLC HSS T3 column (1.8 μm, 2.1 × 100 mm) with 0.1% formic acid in water (A) and acetonitrile (B) as mobile phases. Data were acquired in MSE mode using MassLynx V4.2 with a high-energy range of 10–40 V. ESI conditions included capillary voltage 2500 V (positive) or −2000 V (negative), source temperature 100 °C, and desolvation temperature 500 °C. Raw data were processed in Progenesis QI for peak alignment and normalization, and metabolites were annotated using METLIN and in-house databases. Differential metabolites were identified based on $|FC| > 1.5$, $p < 0.05$, and VIP > 1, and pathway enrichment was conducted using KEGG. PCA, volcano plot, hierarchical clustering heatmap and pathway-associated network analyses were performed to visualize metabolite differences between ultrasound-treated and control samples. Three independent biological replicates were used for each group.

2.14. Statistical analysis

Data analysis was performed using SPSS software (Version 26.0, IBM Corp., USA). All experiments were conducted with independent biological replicates, as indicated in the figure legends. For comparisons between two groups, statistical significance was determined using Student's *t*-test. For comparisons among multiple groups, one-way ANOVA followed by Bonferroni post-hoc multiple comparison test was applied. Significant differences were indicated as $^*p < 0.05$ and $^{**}p < 0.01$. Data were presented as means ± SD unless otherwise stated.

3. Results and discussion

3.1. Enhanced enzymes secretion from T. Reesei incubation with sugarcane bagasse and juice

As two sugarcane cultivars (ROC22 and F134) distinctive at lignocellulose compositions and soluble sugar levels were examined [7], this study initially employed their bagasse and juice samples to co-incubate with a *T. reesei* strain for the secretion of lignocellulose-degrading enzymes (Fig. S1; Fig. 1A). Using previously established methods [18,34], we detected the filter paper (FP) activity of all crude solutions secreted by the *T. reesei* strain incubated with the two sugarcane samples. In comparison, the F134 bagasse-induced sample showed 19% higher FP activity than ROC22 at $p < 0.01$ level (Fig. 1B). While the bagasse was co-supplemented with different dosages of juice squeezed from sugarcane stalks, all samples showed consistently increased FP activities, but the F134 sample showed consistently higher FP activity than that of ROC22 (Fig. 1C). As FP activity serves as a key parameter for cellulose enzymatic digestibility, the significantly higher FP activity induced by F134 reflects its improved recalcitrant properties, such as either significantly reduced cellulose DP value, hemicellulose arabinose proportion and lignin level or much raised cellulose accessibility (Fig. S3). This is consistent with previous findings on the lignocellulose induction, enabling the fungal secretion of biomass-degrading enzymes with high yield and activity [35,36]. Likewise, the F134 samples exhibited consistently higher protein levels than those of the ROC22 samples (Fig. 1D), which was supported by the biomass-degrading enzymes separation under sodium dodecyl sulfate gel profiling (Fig. 1E). By performing individual enzyme assay *in vitro* [18], this study confirmed that all F134 samples had significantly higher BG activities than those of the ROC22 samples across all examined secreted solutions (Fig. S4). Furthermore, the F134 samples retained relatively higher CBHI and EGII activities than the ROC22 samples from either bagasse induction or juice co-supplementation (Fig. S4). In addition, the F134 sample showed higher xylanase activity after co-incubation with 20% juice. Thus, the results indicate that the F134 bagasse could be employed as the optimal substrate for inducing fungal secretion of the lignocellulose-degrading enzymes at high activities while co-supplied with 20% sugarcane juice.

3.2. Optimal ultrasound treatment for improving T. reesei secretion

Given that the selected F134 bagasse effectively induces *T. reesei* secretions of high-activity cellulases and xylanases from 20% sugarcane juice co-incubation as described above, this study aimed to explore an optimal sustainable technology to further enhance enzymes production. As intermittent ultrasound, a typical environmentally friendly treatment, enables cellulases to be unlocked for enhancing biomass enzymatic saccharification [26,37–39], we conducted multiple ultrasound treatments during sugarcane bagasse incubation with *T. reesei* co-supplied with 20% sugarcane juice (Fig. 2). Using different durations and frequencies at three ultrasound intensities, we sorted out the optimal ultrasound condition within the tested treatments, such as 108 W ultrasound for 4 min, repeated three times intermittently. The nominal input energy for this treatment was estimated as 77.8 kJ according to the equation described in Section 2.4.

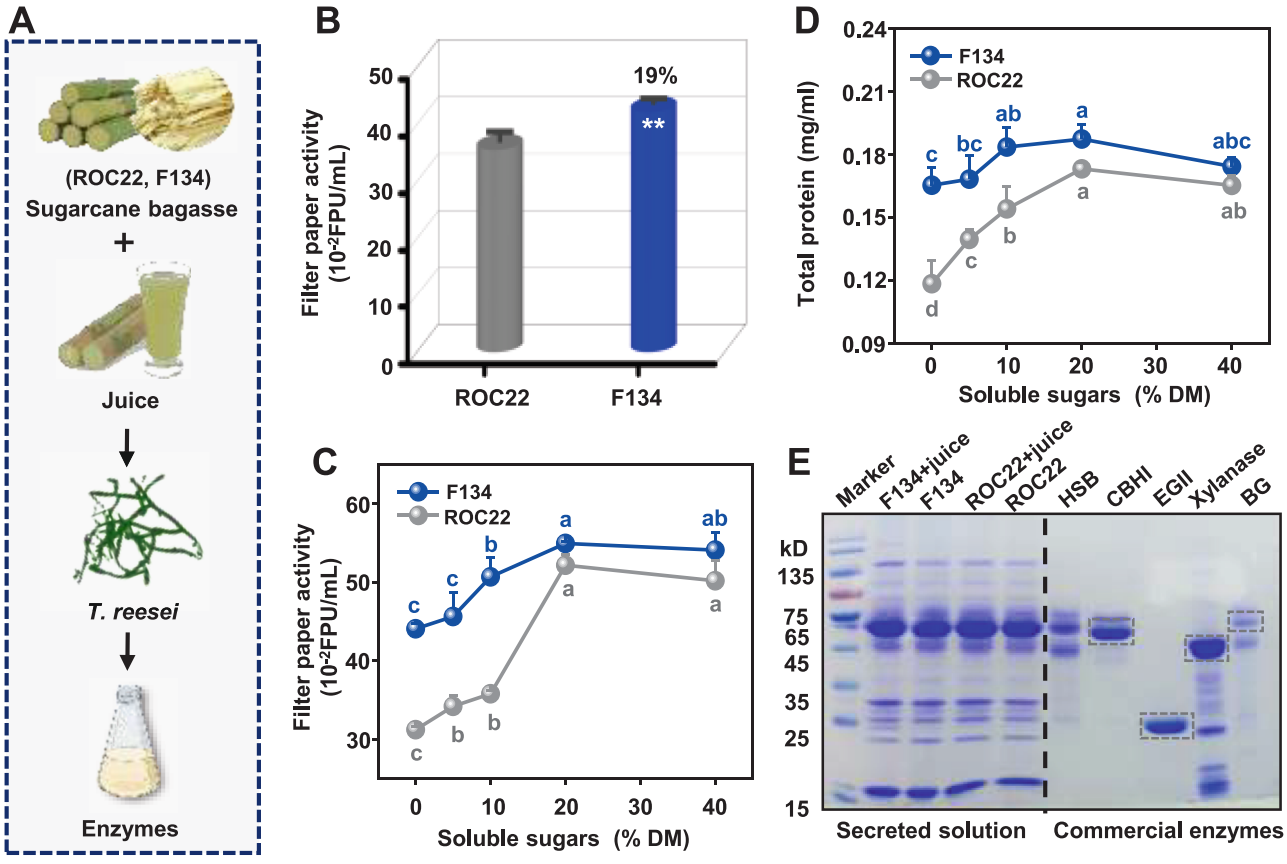

Fig. 1. Characterization of *T. reesei*-secreted enzymes by incubation with two sugarcane bagasse (ROC22, F134) co-suppled with different dosages of sugarcane juice. (A) General experimental procedure; (B) Filter paper activities/FPAs of *T. reesei*-secreted solutions of two sugarcane bagasse samples; (C) The FPAs activities of secreted solutions while co-suppled with different dosages of sugarcane juice; (D) Total protein contents of secreted solutions; (E) SDS-PAGE profiling of secreted solutions co-supplied with 20% sugarcane juice; Lane 1: F134 bagasse supplemented with 20% sugarcane juice; Lane 3: ROC22 bagasse supplemented with 20% sugarcane juice. Dot-boxes highlighted for individual standard (commercial) enzymes as CBHI, EGII, Xylanase and BG; HSB as mixed-cellulases from commercial company; **As significantly raised percentage of F134 sample relative to ROC22 at $p < 0.01$ level (n = 3), bar as means ± SD. Significant differences calculated using one-way ANOVA at $p < 0.05$ (n = 5).

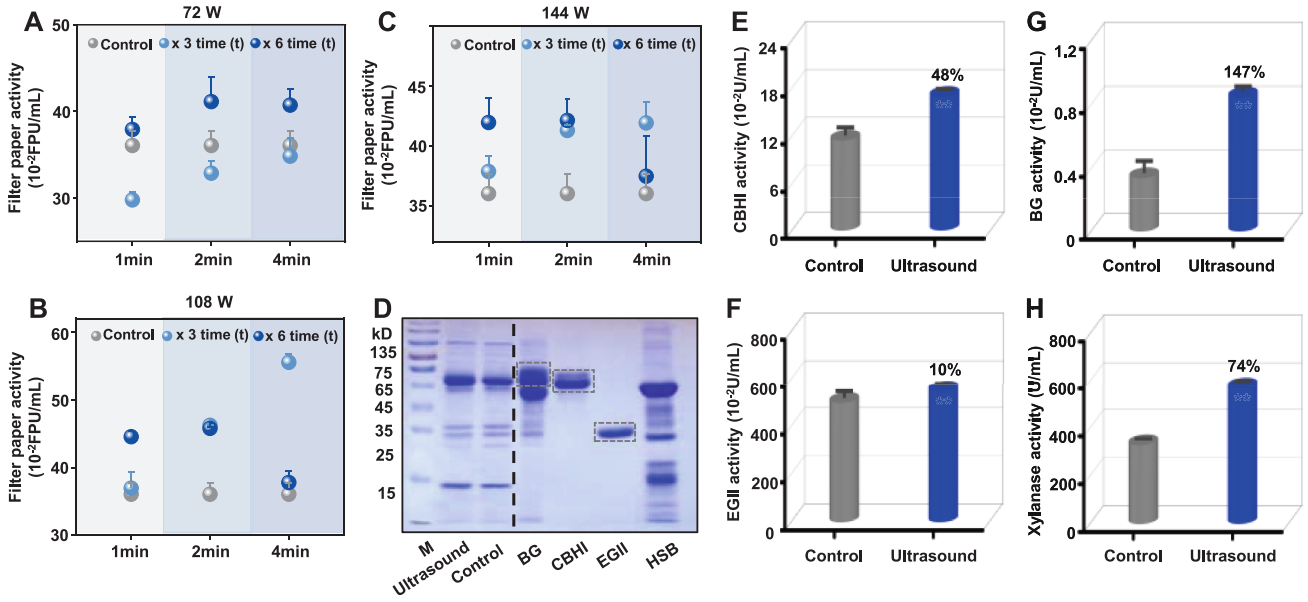

Fig. 2. Intermittent ultrasound treatment of *T. reesei* incubation with F134 sugarcane bagasse co-suppled with 20% sugarcane juice for secreting high-activity enzymes. (A-C) FPAs of secreted solutions under ultrasound treatments at 72,108,144 W power for 1, 2, 4 min under 3 and 6 times (t) repeating, respectively; (D) SDS-PAGE profiling of secreted solutions under the optimal condition (108 W, 4 min, 3 t), Dot-box highlighted as single enzyme; (E-H) Individual enzyme activity (CBHI, EGII, BG and xylanases) assay *in vitro* of the secreted solutions as described (D); **As significantly raised percentage of the optimal ultrasound treatment sample relative to the control (without ultrasound) at $p < 0.01$ level (n = 3), bar as means ± SD.

The calorimetric estimation of the acoustic power delivered to the sample was further performed to improve ultrasound characterization and reproducibility under the same sonication configuration applied in the cultivation experiments (Fig. S2; Table S2). Under the nominal settings of 72, 108 and 144 W, the temperature rise of the 30 mL liquid sample over 120 s was 3.0 ± 0.30, 3.8 ± 0.26 and 4.4 ± 0.53 °C, respectively, being corresponding to calorimetrically-estimated acoustic powers of 3.14 ± 0.31, 3.98 ± 0.28 and 4.60 ± 0.55 W. These results confirmed that the actual sample-level acoustic power delivered by the sonication was substantially lower than the nominal setting, as expected for flask-mediated sonication. For the optimized condition, the acoustic energy density was estimated as 0.133 ± 0.009 W/mL and the total delivered acoustic energy was 2863.2 ± 199.4 J. This treatment increased the FP activity by 54% compared to the control (no ultrasound treatment) (Fig. 2A-C). This optimal ultrasound condition may reflect a balance between beneficial and adverse cavitational effects, because moderate cavitation can improve liquid mixing, mass transfer and fungal-substrate contact, whereas excessive cavitation may generate strong shear forces, localized heating or free radicals that could damage fungal hyphae or reduce enzyme stability [40,41]. Moreover, we detected individual enzyme activity *in vitro* for four major mixed-cellulases: CBHI, EGII, BG, and xylanase (Fig. 2D-H). Consequently, all four major enzyme activities were significantly increased by the optimal ultrasound treatment at $p < 0.01$ level (n = 3) relative to the control. In particular, the BG activity was significantly increased up to 1.47-fold from the optimal ultrasound treatment, compared to the other three enzymes examined. As BG is the rate-limiting enzyme in cellulases cocktails [14,18,19], the remarkably high BG activity should be one of major causes for consistently enhanced biomass saccharification examined in this study. Notably, this study compared the five individual enzymes activities with the previously reported ones under chemicals and enzyme treatments (Table 1). As a comparison, the *T. reesei* under ultrasound treatment could secret much higher BG and xylanase activities than the chemical treatments, but its CBHI and EGII activities were relatively lower [17,42–44], suggesting the specific roles of ultrasound treatments for producing high-activity BGs and xylanases as an environmentally-friendly alternative. Particularly, the ultrasound treatment caused the *T. reesei* secreting the FPA at the highest activity as previously reported from Mn^{2+} treatment. In addition, the *T. reesei*-secreted enzymes under optimal ultrasound treatment were dissected by LC-MS/MS assay. As a result, about six types of lignocellulose-degradation enzymes were examined including cellobiohydrolases, *endo*-β-1,4-glucanases, β-glucosidase, *endo*-1,4-β-xylanases, xyloglucanase, swollenin (Table 2; Fig. S5 and S6), suggesting the secreted enzymes complexes should be sufficient for biomass enzymatic saccharification in bioenergy crops as described below. Therefore, the optimal ultrasound treatment could effectively enhance the *T. reesei* secretion of lignocellulose-degradation enzymes at high activities.

3.3. Distinct impacts on T. reesei incubation under optimal ultrasound treatment

To elucidate the improved secretion of lignocellulose-degrading enzymes from *T. reesei* incubation under the optimal ultrasound treatment

Table 1
Comparison of the *T. reesei*-secreted enzymes achieved in this study and from previous works.

Treatments	FPA (%)	CBHI activity (%)	EGII activity (%)	BG activity (%)	Xylanases activity (%)	References
Ultrasound	**54**[#]	**48**	**10**	**147**	**74**	**This study**
H_2O_2	25	–[*]	19	–	–	Zhao et al2018
Enzymatic hydrolysis	54	43	56	20	13	Li et al 2019
Ca^{2+}	–	40	80	–	40	Chen et al 2016
Rapamycin	22	20	15	–	–	Pang et al 2021

[#] As increased rates of enzymatic activities by inducing substrate compared to the control (without ultrasound treatments);
[*] Data as not detectable.

Table 2
LC-MS/MS analyses of *T. reesei*-secreted enzymes incubated with F134 sugarcane bagass co-supplied with 20% sugarcane juice under optimal ultrasound treatments.

Protein Name	Accession No.	Coverage [%]	Peptides	Razor + unique peptides	Unique peptides	Intensity A	MW [kDa]
Cellobiohydrolase I	A0A024RXP8	10.12	4	4	4	1,419,200	54.11
Cellobiohydrolase II	A0A024SH76	9.34	4	4	4	37415.4	49.65
Endo-β-1,4-glucanase I	A0A024SNB7	2.83	1	1	1	440,030	48.21
Endo-β-1,4-glucanase VII	A0A024SFJ2	2.81	1	1	1	4322.09	26.80
β-glucosidase I	A0A024SB94	3.33	2	2	2	1149.04	84.68
Endo-1,4-β-xylanase I	P36218	7.42	1	1	1	3188.09	24.58
Endo-1,4-β-xylanase II	P36217	6.73	1	1	1	78471.3	24.07
Endo-1,4-β-xylanase III	A0A024SIB3	2.88	1	1	1	3254.12	38.08
Xyloglucanase	A0A024S9Z6	9.31	7	7	7	139,640	87.13
Swollenin	A0A024RZP7	3.45	2	2	2	141,769	51.52

performed, we further measured the release of hexoses and pentoses from the supernatants of *T. reesei* incubation with sugarcane bagasse and juices (Fig. 3A-B; Fig. S7). During the *T. reesei* incubation from 3 d to 7 d, the optimal ultrasound treatment consistently caused significantly more hexoses and pentoses release by 8%-28% at $p < 0.01$ (n = 3) compared to the control (without ultrasound), which should be resulted from the improved sugarcane bagasse digestion of *T. reesei*-secreted enzymes. These findings were also corroborated by the significantly increased total protein levels in the supernatants ranging from 19% to 31% under the optimal ultrasound treatment (Fig. 3C). Meanwhile, we observed a gradual reduction in the interfacial tension trend of the supernatant under the optimal ultrasound treatment relative to the control (Fig. 3D), which should account for the significantly higher contents of proteins and soluble sugars (hexoses and pentoses) examined in the ultrasound treatment. Furthermore, this study detected the cellulose CrI of the solid bagasse residues during *T. reesei* incubation. The optimal ultrasound treatment consistently yielded significantly lower CrI values than those of the control (Fig. 3E), which should be mainly due to the improved enzymatic hydrolysis of crystalline cellulose in the ultrasound-treated sugarcane bagasse samples. To confirm this finding, we applied Fourier transform infrared spectroscopy to detect the chemical linkages in the solid bagasse residues after *T. reesei* incubation for 7 d (Fig. 3F). In comparison with the raw material of sugarcane bagasse, the two solid residues from *T. reesei* incubation exhibited changes in four peaks corresponding to the C-H_2, C-O-C, and C–H chemical groups (897, 1045, 1164, 1368 cm^{-1}) associated with lignocellulose interlinkages (Table S3), indicating that lignocellulose digestion of sugarcane bagasse occurred during *T. reesei* incubation [45–50]. However, the four peaks of the optimal ultrasound treatment sample were more altered than those of the control, consistent with either its reduced CrI and interfacial tension values or raised sugars and protein levels. Hence, these results suggest that the optimal ultrasound treatment could not only enhance the *T. reesei* secretion of biomass-degrading enzymes, but it should also facilitate the enzymatic digestion of sugarcane bagasse substrate into soluble sugars as carbon source for feedback-like improvement of *T. reesei* secretion.

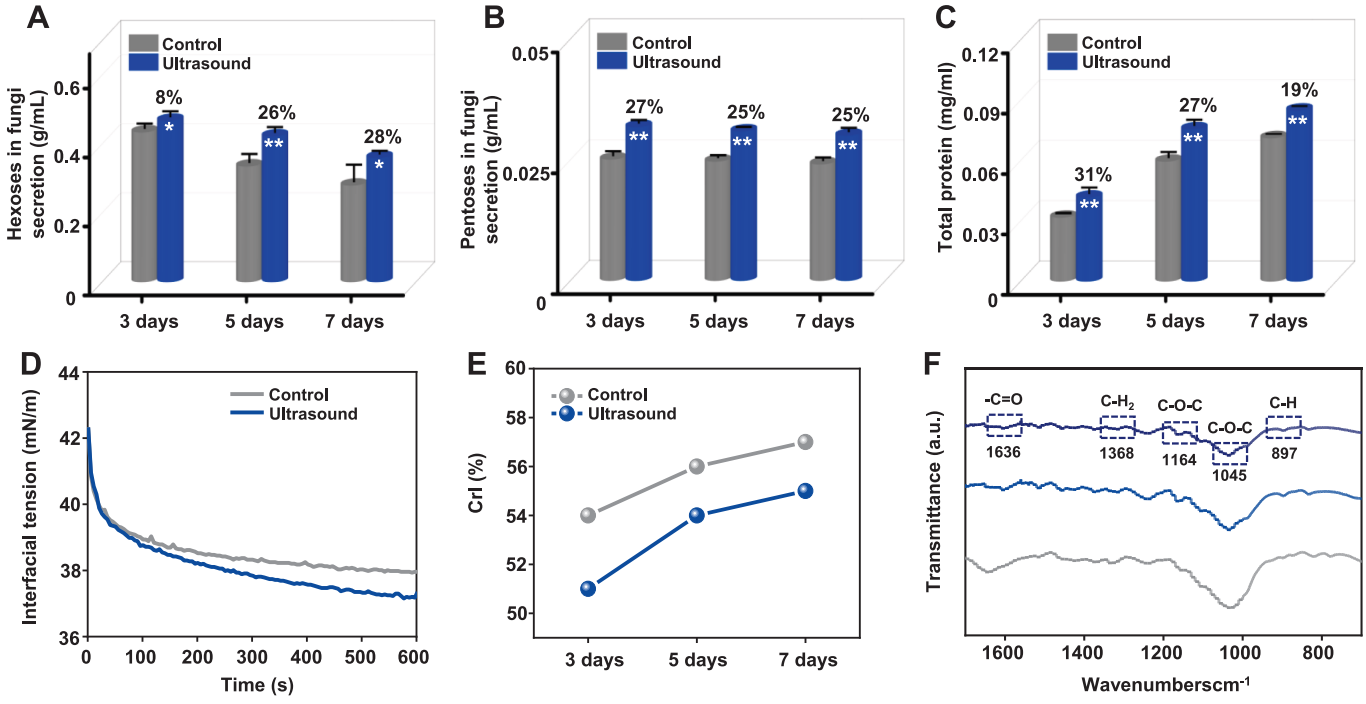

Fig. 3. Characterization of *T. reesei* incubation with F134 sugarcane bagasse co-suppled with 20% sugarcane juice under optimal ultrasound treatment (108 W, 4 min, 3 t). (A-B) Hexoses and pentoses levels of secreted solutions after intermittent ultrasound treatments for 3-, 5-, 7-days incubations; (C) Total protein contents of secreted solutions; (D) Dynamic interfacial tensions of secreted solutions after 7-day incubation; (E) Crystalline index (CrI) values of lignocellulose residues after 7-day incubation; (F) FT-IR profiling of lignocellulose residues after 7-day incubation; Dot-box highlighted for altered peak as annotated in Table S3, grey as raw lignocellulose material without incubation with *T. reesei*, light blue as lignocellulose residue after 7-day induction without ultrasound, dark blue as residue after optimal ultrasound treatment for 7-day incubation; **As significantly raised percentage of the optimal ultrasound treatment relative to the control (without ultrasound) at $p < 0.01$ level (n = 3), bar as means ± SD.

3.4. *T. reesei* hyphal fragmentation and lignocellulose homogeneity under optimal ultrasound treatment

To understand the optimal ultrasound treatment role in *T. reesei* incubation with sugarcane bagasse for high-activity enzymes secretion, we observed the sugarcane bagasse substrate and *T. reesei* growth during a time-course incubation (Fig. 4A). After incubation for 3 days after optimal ultrasound treatment, the bagasse substrates exhibited much more reduced dimensions comparted to the control (without ultrasound). After 7 days incubation, the bagasse substrates became much smaller and even more homogeneous than those of the control. Meanwhile, this study observed drastic hyphal fragmentation of *T. reesei* from 3 days incubation after optimal ultrasound treatment, and the hyphae remained small from 7 days incubation. By comparison, the *T. reesei* without ultrasound treatment showed a normal growth to form larger and rich hyphae from 3 days to 7 days incubation. During 3–7 days cultivations, the optimal ultrasound treatments could consistently reduce either the lengths of *T. reesei* hyphae or the sizes of bagasse substrates by 32%-67% relative to the controls (Fig. 4B and C). Since the bagasse substrates became remarkably smaller residues at higher homogeneity and the hyphae were fragmented with evenly distributed under longer incubation after optimal ultrasound treatment, it should facilitate the *T. reesei* interaction with lignocellulose for effectively improving enzymes secretion, which was consistent with significantly raised hexoses and pentoses released from the *T. reesei* incubation under optimal ultrasound treatment (Fig. 3). As ultrasound is functional for effective separation of lignocellulose [26,51,52], the formation of smaller bagasse residues at high homogeneity was mainly due to both

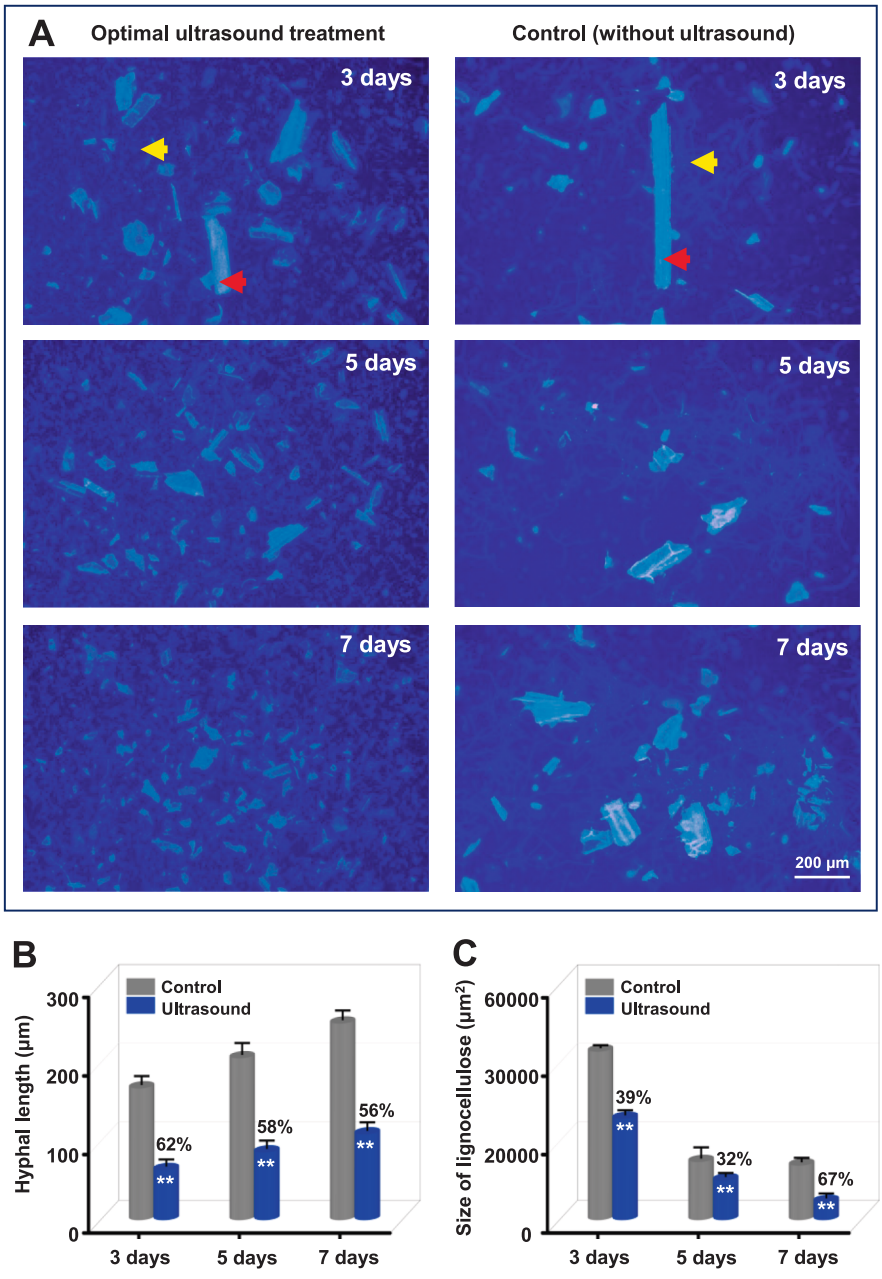

Fig. 4. Time course observations of *T. reesei* incubations under the optimal ultrasound treatments. (A) Fluorescence images of lignocellulose residues (red arrow) and hyphae tissues (yellow arrow) from *T. reesei* incubation with sugarcane bagasse (F134) co-supplied with 20% sugarcane juice after the optimal ultrasound treatment as described in Fig. 2; (B) Average length of randomly-selected 30 hyphae (n = 30); (C) Average size of randomly-selected 30 lignocellulose substrates (n = 30). **As significant difference between ultrasound treatment and control at $p < 0.01$ level, bar as means ± SD.

optimal ultrasound treatment and lignocellulose digestion of *T. reesei*-secreted enzymes during long time incubation, which should be the major cause accounting for *T. reesei* secretion of lignocellulose-degradation enzymes at high activities and high yields as detected above. Furthermore, this study performed independent ultrasound pretreatment with either a *T. reesei* strain only or a sugarcane bagasse substrate only before incubation for 7 days (Fig. S8). In comparison with the control (without ultrasound), the ultrasound pretreatment could not significantly alter FPAs and total protein levels in the two samples examined. Even though multiple ultrasound treatments were performed before *T. reesei* incubation with sugarcane bagasse co-supplied with 20% sugarcane juice, both the FPAs and total protein levels were not significantly improved compared to the control (Fig. S9). The results suggested that the enhanced enzyme production under the optimal ultrasound treatment should be more associated with the ultrasound-assisted coincubation process involving hyphal fragmentation, substrate homogenization and increased fungal-substrate contact. To further estimate whether fungal biomass-associated accumulation was also changed under the optimal ultrasound treatment, we measured ergosterol in the fungal-lignocellulosic residues after 7-day incubation as an indirect fungal biomass proxy (Fig. S10). In comparison with the control (without ultrasound), the ultrasound-treated sample showed a significantly higher ergosterol content, which was increased from 75.6 ± 6.6 to 107.5 ± 18.6 μg/g dry weight. The data suggested that the optimal ultrasound treatment should be associated with a higher fungal biomass-related signal in the incubation system. Nevertheless, mild physical stress, partial cellular disruption or stress-related secretion responses could not be completely excluded.

3.5. Enhanced biomass saccharification of major bioenergy crops using *T. reesei*-secreted enzymes

By employing alkali-pretreated lignocellulose substrates as previously obtained in rice, eucalyptus and fern [53–55], this study detected their biomass saccharification by calculating the yields of hexoses (% cellulose) and total sugars (pentoses and hexoses) (% dry matter) released from the enzymatic hydrolyses of *T. reesei*-secreted enzymes (Fig. 5A). Using the *T. reesei*-secreted enzymes hydrolyses under optimal ultrasound treatment, the three bioenergy crops showed significantly increased hexoses by 64%, 50% and 53% at $p < 0.01$ level (n = 3), compared to the control enzymes without ultrasound (Fig. 5B). Likewise, the total sugars yields were respectively increased by 43%, 42% and 34% in three bioenergy crops under the optimal ultrasound treatment relative to the control (Fig. 5C, Fig. S11). These were thus consistent with the findings that optimal ultrasound treatment improved the secretion of the four major enzymes examined above by *T. reesei* (Fig. 2). Notably, even though without ultrasound treatment, the *T. reesei*-secreted enzymes retained relatively higher hexoses and total sugars yields than those of the commercial enzymes (HSB), confirming that our sugarcane bagasse and juice are the optimal substrates for inducing the fungal secretion of biomass-degrading enzymes at higher activities. Despite the comparison with commercial HSB was performed under the same FP activity loading, it should not indicate an identical enzyme composition or accessory protein abundance. Therefore, the higher sugar release observed using the ultrasound-derived enzyme preparation should be mainly due to improved hydrolysis performance under equal cellulase activity loading.

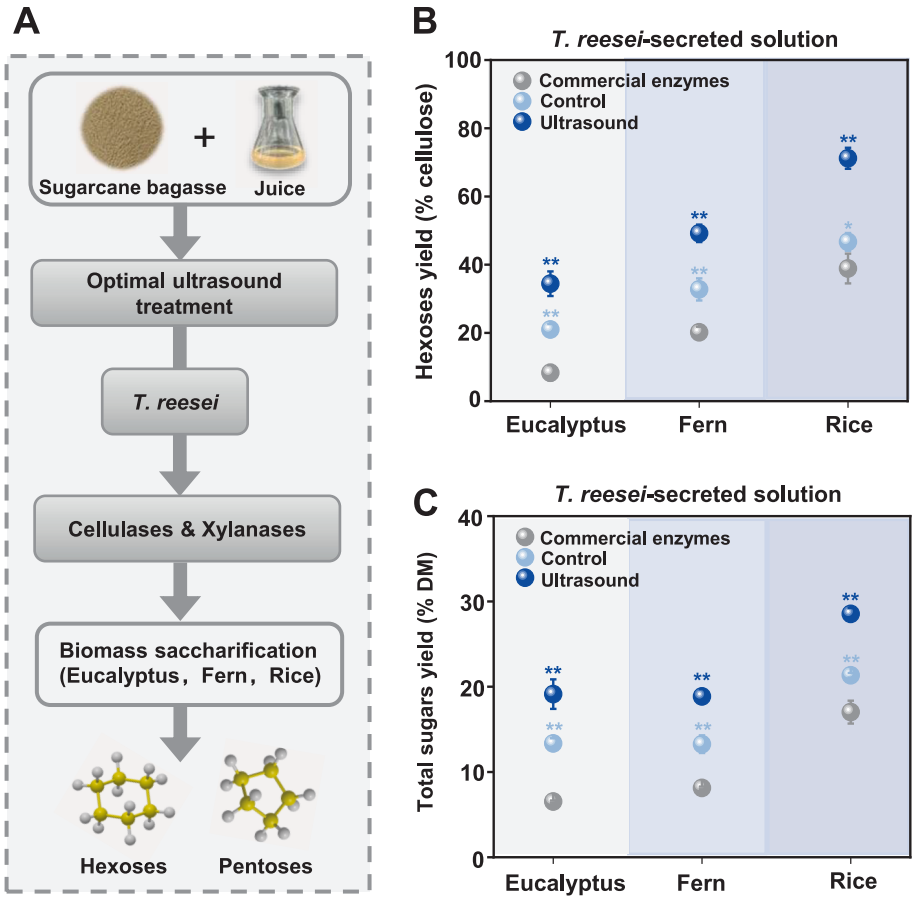

Fig. 5. Enhanced biomass enzymatic saccharification of three bioenergy crops (rice, eucalyptus, fern) using *T. reesei*-secreted solutions under optimal ultrasound treatments. (A) General experimental procedure; (B, C) Hexoses and total sugars yields released from enzymatic hydrolyses of 0.5% NaOH-pretreated lignocelluloses; * and **As significantly raised percentages of the optimal ultrasound sample relative to the control (without ultrasound) or the control relative to the commercial enzyme at $p < 0.05$ and 0.01 levels (n = 3), bar as means ± SD.

3.6. Metabolomic remodeling of T. reesei incubation under optimal ultrasound treatment

To clarify how the optimal ultrasound treatment affected the metabolic pathways of *T. reesei* incubation with sugarcane bagasse, we performed untargeted metabolomic profiling using the whole system including fungal-secreted enzymes in supernatant and all remaining fungal-lignocellulose residues after 7-day incubation. Regarding the PCA score plots, the ultrasound-treated samples were obviously separated from the control (without ultrasound) samples in both secreted enzymes and remaining residues, with PC1 and PC2 explaining 53.55% and 14.16% of the total variation in the enzymes, and 53.22% and 14.07% in residues, respectively (Fig. 6A and B). The data suggest that the optimal ultrasound treatment could induce a broad metabolic shift in the whole system of *T. reesei*-bagasse incubation. Consistently, the volcano plot analysis detected 226 differential metabolites in the enzymes, including 138 up-regulated and 88 down-regulated metabolites, whereas 228 differential metabolites were identified in the residues, including 118 up-regulated and 110 down-regulated metabolites (Fig. 6C and D). The hierarchical clustering heatmaps showed distinct accumulation patterns of differential metabolites between the control and ultrasound-treated samples in both enzymes and residues, confirming a distinctively altered metabolic remodeling caused by ultrasound treatment (Fig. S12 and S13). KEGG enrichment analysis further revealed that the differential metabolites in the enzymes were mainly enriched in linoleic acid metabolism, biosynthesis of unsaturated fatty acids, cutin, suberin and wax biosynthesis, purine metabolism, pyrimidine metabolism, flavonoid biosynthesis and lysine degradation, together with several database-annotated secondary pathways (Fig. 7A). In the residues, the differential metabolites were enriched in linoleic acid metabolism, arachidonic acid metabolism, cAMP signaling pathway, purine metabolism, pentose phosphate pathway, glycerophospholipid metabolism, biosynthesis of unsaturated fatty acids, and cutin, suberin and wax biosynthesis (Fig. 7B). Those enriched pathways were mainly associated with changes in lipid-associated metabolism, nucleotide metabolism and carbohydrate-associated metabolic processes, which should be relevant to *T. reesei* interaction with lignocellulose residues [56]. In particular, the enrichment of the pentose phosphate pathway in the residues was consistent with the enhanced release of pentoses, whereas the enrichment of lipid- and fatty-acid-related pathways suggested possible changes in the soluble and residue-associated microenvironment. Furthermore, the pathway-associated networks highlighted several representative enriched pathways and differential metabolites in both enzymes and residues, supporting that ultrasound treatment could reshape the enzyme fraction and the residue-associated metabolite profile (Fig. S14). In terms of increased soluble sugars, higher protein secretion, reduced interfacial tension, decreased cellulose CrI and more homogeneous substrate

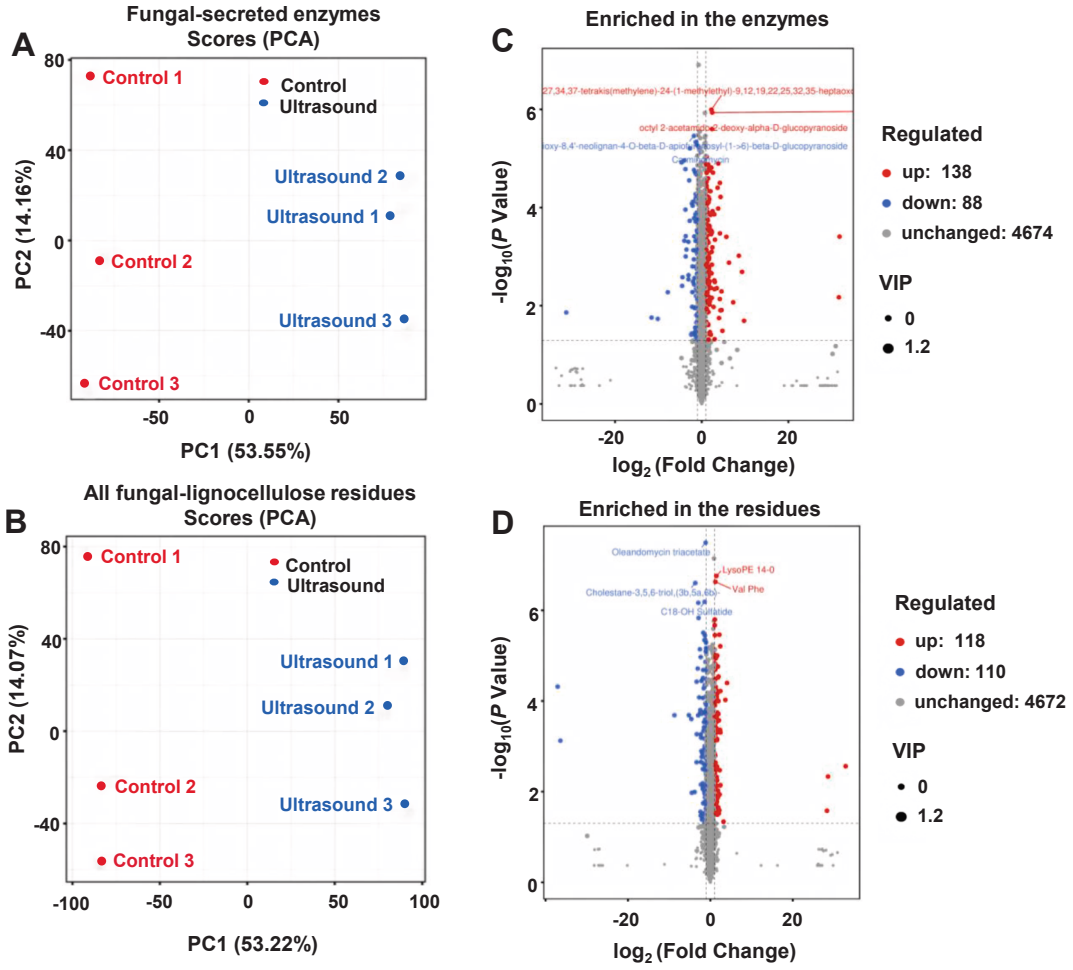

Fig. 6. Metabolomic analyses of the fungal-secreted enzymes of supernatant and all remaining fungal-lignocellulose residues from *T. reesei* incubation under the optimal ultrasound treatment. (A, B) PCA score plots of metabolites relative to the control (without ultrasound); (C, D) Volcano plots of differential metabolites between ultrasound-treated and control samples. Each point represents a metabolite based on its $\log_2$-transformed fold change (x-axis) and $-\log_{10}$-transformed *p*-value (y-axis); Red and blue dots indicate up- and down-regulated metabolites; grey dots indicate unchanged metabolites. The color scale indicates VIP values.

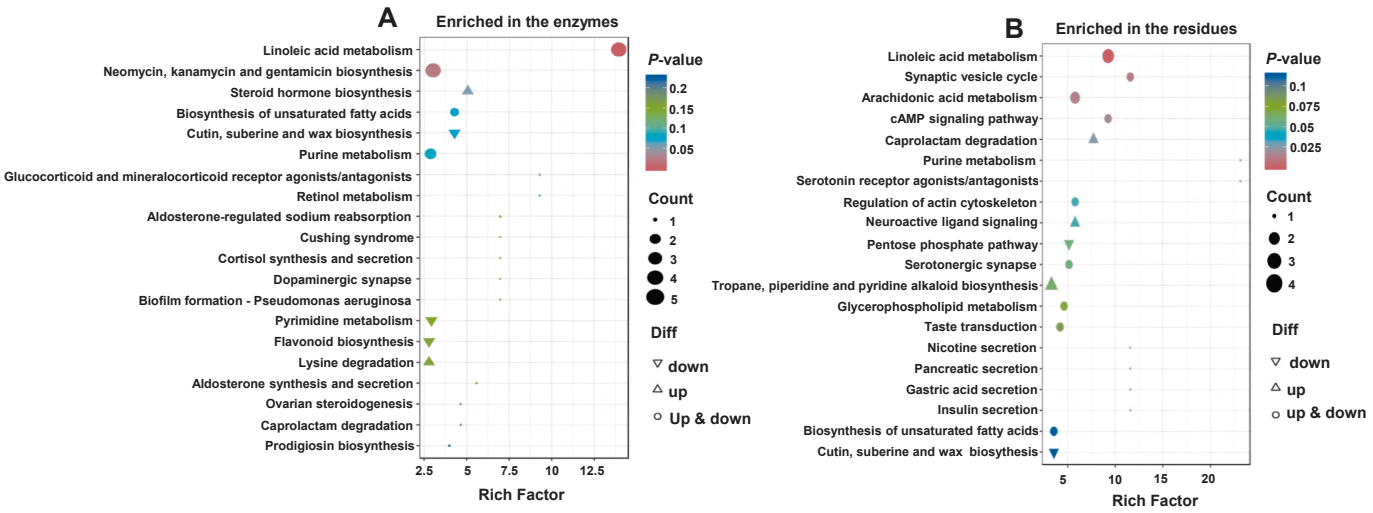

Fig. 7. KEGG pathway enrichment analysis of differential metabolites detected in the fungal-secreted enzymes and all remaining fungal-lignocellulose residues from *T. reesei* incubation under the optimal ultrasound treatment. (A) Secreted enzymes; (B) Remaining residues. Each bubble represents a specific KEGG pathway and the Rich Factor (x-axis) indicates the proportion of differentially enriched metabolites mapped to a given pathway; The bubble size corresponds to the number of metabolites within the pathway, and the color intensity represents the *P*-value from the enrichment analysis.

digestion as described above, the metabolomic evidence was consistent with altered whole-system metabolic remodeling and the changes of incubation microenvironment under optimal ultrasound treatment, which should mainly contribute to the enhanced secretion of lignocellulose-degrading enzymes. Because the metabolomic samples were collected from the enzymes and lignocellulose residues rather than

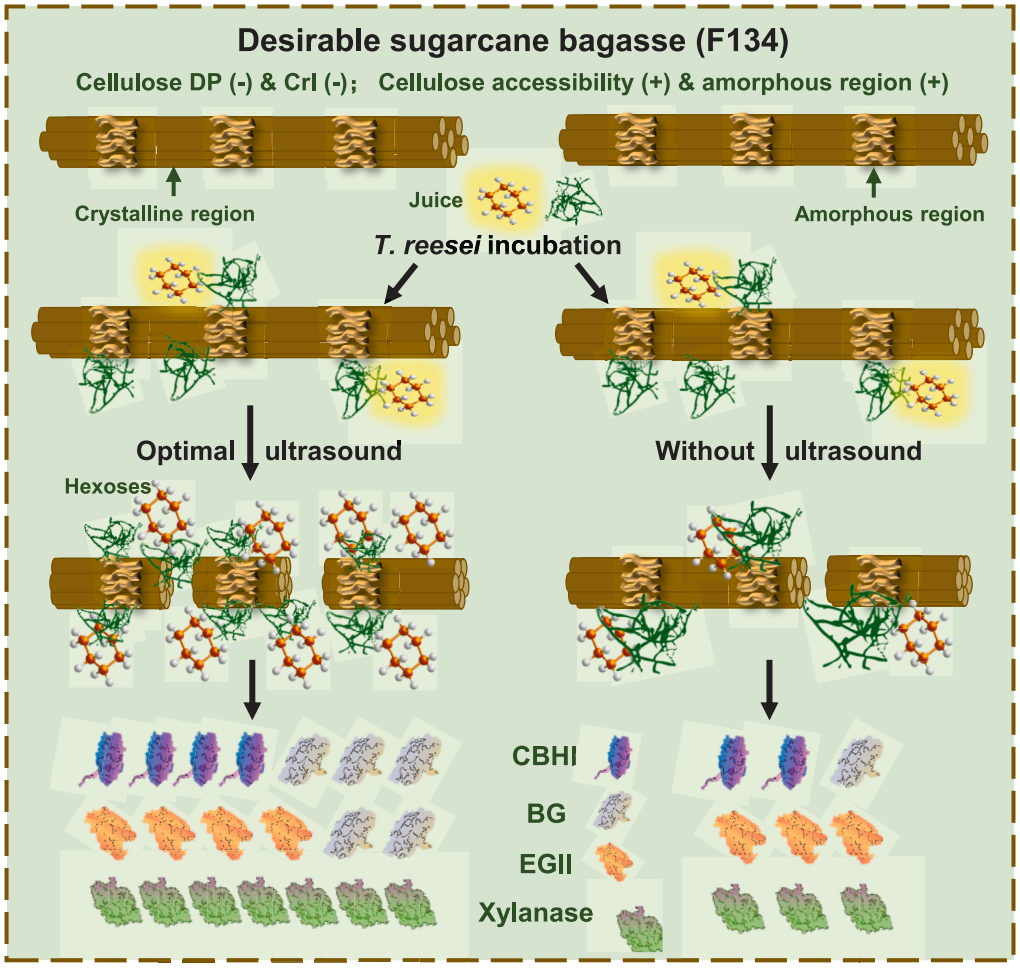

Fig. 8. A working model of optimal ultrasound treatment for enhancing *T. reesei* interaction with selected sugarcane bagasse substrates co-supplied with juice to secret lignocellulose-degradation enzymes at high activities. (−) and (+) As relatively reduced and raised cellulose features.

purified fungal cells, those obtained data should be defined as altered metabolic remodeling of the whole incubation environment.

3.7. A working model of optimal ultrasound treatment for t. Reesei secreting high-activity enzymes

Based on the major findings achieved in this study, we developed a working model to illustrate the enhanced secretion of distinct cellulases and xylanases through optimal ultrasound treatments during selected sugarcane bagasse incubation with *T. reesei* (Fig. 8). As the F134 sugarcane bagasse has been characterized by significantly reduced lignocellulose recalcitrant factors (low cellulose DP and CrI values) accountable for relatively increased cellulose accessibility and amorphous cellulose chains [1,7,20,57,58], it is assumed that the *T. reesei* strain should initially attack the amorphous cellulose regions of sugarcane bagasse to release cellulases and xylanases [18]. Meanwhile, the co-supplied sugarcane juice can be used as the initial carbon source to activate fungi attacks. Because the ultrasound could physically fragment the hyphae and lignocellulose substrates, it is likely that the optimal ultrasound treatment drastically facilitated the interactions between the hyphal fragmentation at well-distribution and the digested bagasse substrates at high-homogeneity, which enhances *T. reesei* secretion of the lignocellulose-degradation enzymes, in particular for three major types of enzymes (CBHIs, EGs, xylanases). This enhancement should consequently be involved in lignocellulose digestion to release hexoses and pentoses as a step-carbon source for consistently activating *T. reesei* secretion. Significantly, the fungal-secreted enzymes led to much enhanced biomass saccharification of three representative bioenergy crops even under mild alkali pretreatment. Nevertheless, it remains to explore if the optimal ultrasound treatment is also effective for enhancing enzymes productions from other fungi strains. The transcriptomic and proteomic profiling of fungal induction and secretion during ultrasound-treated incubations would further elucidate the specific metabolic pathways and genetic regulatory networks in fungi strains in the future.

4. Conclusions

This study demonstrated that incubating sugarcane bagasse with digestible lignocellulose along with sugarcane juice co-supplementation, effectively induced *T. reesei* secretion of higher activities of biomass-degrading enzymes. By exploring the optimal ultrasound treatments for *T. reesei* incubation, improvements in cellulases and xylanases activities were much extended for distinctively enhanced biomass enzymatic saccharification even under mild alkali pretreatments in representative bioenergy crops. Notably, the optimal ultrasound treatment was highly associated with hyphal fragmentation, homogenously-digested lignocellulose substrates and altered whole-system metabolomic remodeling, suggesting an improved interaction between *T. reesei* and bagasse substrate. Based on the calorimetric characterization, this study further supported an experimentally-validated process association among the sonication treatment, hyphal fragmentation, substrate homogenization and enhanced extracellular enzyme performance, but a fully established-biological regulatory mechanism remains to test in the future. Nonetheless, this study proposes a working model for optimal ultrasound roles in *T. reesei* incubation with bagasse substrate for secretion of a cellulase complex at high-yield and high-activity, providing an advanced ultrasound technology for fungal enzyme production and biomass enzymatic saccharification in bioenergy crops.

CRediT authorship contribution statement

Hao Peng: Writing – original draft, Methodology, Investigation, Formal analysis. **Jingyuan Liu:** Writing – review & editing, Investigation, Formal analysis. **Jiale Liu:** Methodology, Investigation, Formal analysis. **Xueyu Wang:** Methodology, Investigation, Formal analysis. **Hailang Wang:** Methodology, Investigation, Formal analysis. **Huan Ma:** Methodology, Investigation, Formal analysis. **Yansong Fu:** Methodology, Investigation, Formal analysis. **Dan Sun:** Methodology, Investigation, Formal analysis. **Yanting Wang:** Validation, Supervision, Funding acquisition. **Chunxiang Fu:** Validation, Supervision, Funding acquisition. **Liangcai Peng:** Validation, Supervision, Funding acquisition. **Peng Liu:** Writing – review & editing, Supervision, Methodology, Conceptualization.

Declaration of competing interest

The authors declare that they have no known competing financial interests or personal relationships that could have appeared to influence the work reported in this paper.

Acknowledgments

This work was in part supported by Hubei Provincial Natural Science Foundation of China for Excellent Young Scientists (2024AFA100), the National Natural Science Foundation of China (32470273, 32170268, 32101701), the National 111 Project of the Ministry of Education of China (D17009), and the Initiative Grant of Hubei University of Technology for High-level Talents (GCC20230001).

Appendix A. Supplementary data

Supplementary data to this article can be found online at https://doi.org/10.1016/j.ultsonch.2026.107905.

References

[1] Y. Ai, H. Wang, P. Liu, H. Yu, M. Sun, R. Zhang, J. Tang, Y. Wang, S. Feng, L. Peng, Insights into contrastive cellulose nanofibrils assembly and nanocrystals catalysis from dual regulations of plant cell walls, Sci. Bull. 69 (2024) 3815–3819.
[2] M. Wang, Y. Wang, J. Liu, H. Yu, P. Liu, Y. Yang, D. Sun, H. Kang, Y. Wang, J. Tang, C. Fu, L. Peng, Integration of advanced biotechnology for green carbon, Green Carbon. 2 (2024) 164–175.
[3] H. Hu, R. Zhang, Z. Tao, X. Li, Y. Li, J. Huang, X. Li, X. Han, S. Feng, G. Zhang, L. Peng, Cellulose synthase mutants distinctively affect cell growth and cell wall integrity for plant biomass production in *Arabidopsis*, Plant Cell Physiol. 59 (2018) 1144–1157.
[4] L. Zhao, D. Zhao, Hydrolyzed polyacrylamide biotransformation during the formation of anode biofilm in microbial fuel cell biosystem: bioelectricity, metabolites and functional microorganisms, Bioresour. Technol. 360 (2022) 127581.
[5] M.M. Kininge, P.R. Gogate, Intensification of alkaline delignification of sugarcane bagasse using ultrasound assisted approach, Ultrason. Sonochem. 82 (2022) 105870.
[6] L.P.S. Vandenberghe, K.K. Valladares-Diestra, G.A. Bittencourt, L.A. Zevallos Torres, S. Vieira, S.G. Karp, E.B. Sydney, J.C. de Carvalho, V. Thomaz Soccol, C. R. Soccol, Beyond sugar and ethanol: the future of sugarcane biorefineries in Brazil, Renew. Sustain. Energy Rev. 167 (2022) 112721.
[7] Y. Fu, H. Gao, H. Yu, Q. Yang, H. Peng, P. Liu, Y. Li, Z. Hu, R. Zhang, J. Li, Z. Qi, L. Wang, L. Peng, Y. Wang, Specific lignin and cellulose depolymerization of sugarcane bagasse for maximum bioethanol production under optimal chemical fertilizer pretreatment with hemicellulose retention and liquid recycling, Renew. Energ. 200 (2022) 1371–1381.
[8] J. Jia, B. Yu, L. Wu, H. Wang, Z. Wu, M. Li, P. Huang, S. Feng, P. Chen, Y. Zheng, L. Peng, Biomass enzymatic saccharification is determined by the non-KOH-extractable wall polymer features that predominately affect cellulose crystallinity in corn, PLoS One 9 (2014) e108449.
[9] Z. Hu, H. Peng, J. Liu, H. Zhang, S. Li, H. Wang, Z. Lv, Y. Wang, D. Sun, J. Tang, L. Peng, Y. Wang, Integrating genetic-engineered cellulose nanofibrils of rice straw with mild chemical treatments for enhanced bioethanol conversion and bioaerogels production, Ind. Crops Prod. 202 (2023) 177044.
[10] S. Chatterjee, S.V. Mohan, Simultaneous production of green hydrogen and bioethanol from segregated sugarcane bagasse hydrolysate streams with circular biorefinery design, Chem. Eng. J. 425 (2021) 130386.
[11] M.C. Nwamba, G. Song, F. Sun, M.R. Mukasekuru, H. Ren, Q. Zhang, T. Cao, H. Wang, H. Sun, J. Hong, Efficiency enhancement of a new cellulase cocktail at low enzyme loading for high solid digestion of alkali catalyzed atmospheric glycerol organosolvent pre-treated sugarcane bagasse, Bioresour. Technol. 338 (2021) 125505.
[12] L. Wu, M. Li, J. Huang, H. Zhang, W. Zou, S. Hu, Y. Li, C. Fan, R. Zhang, H. Jing, L. Peng, S. Feng, A near infrared spectroscopic assay for stalk soluble sugars,

bagasse enzymatic saccharification and wall polymers in sweet sorghum, Bioresour. Technol. 177 (2015) 118–124.
[13] R. Zhang, H. Gao, Y. Wang, B. He, J. Lu, W. Zhu, L. Peng, Y. Wang, Challenges and perspectives of green-like lignocellulose pretreatments selectable for low-cost biofuels and high-value bioproduction, Bioresour. Technol. 369 (2023) 128315.
[14] P. Liu, Y. Wang, H. Kang, Y. Wang, H. Yu, H. Peng, B. He, C. Xu, K. Jia, S. Liu, T. Xia, L. Peng, Upgraded cellulose and xylan digestions for synergistic enhancements of biomass enzymatic saccharification and bioethanol conversion using engineered *Trichoderma reesei* strains overproducing mushroom LeGH7 enzyme, Int. J. Biol. Macromol. 278 (2024) 134524.
[15] N. Shibata, H. Kakeshita, K. Igarashi, Y. Takimura, Y. Shida, W. Ogasawara, T. Koda, T. Hasunuma, A. Kondo, Disruption of alpha-tubulin releases carbon catabolite repression and enhances enzyme production in *Trichoderma reesei* even in the presence of glucose, Biotechnol. Biofuels 14 (2021) 39.
[16] T. Kogo, Y. Yoshida, K. Koganei, H. Matsumoto, T. Watanabe, J. Ogihara, T. Kasumi, Production of rice straw hydrolysis enzymes by the fungi *Trichoderma reesei* and *Humicola insolens* using rice straw as a carbon source, Bioresour. Technol. 233 (2017) 67–73.
[17] A. Pang, H. Wang, F. Zhang, X. Hu, F. Wu, Z. Zhou, W. Wang, Z. Lu, F. Lin, High-dose rapamycin exerts atemporary impact on *T. reesei* RUT-C30 through gene *trFKBP12*, Biotechnol. Biofuels 14 (2021) 77.
[18] P. Liu, A. Li, Y. Wang, Q. Cai, H. Yu, Y. Li, H. Peng, Q. Li, Y. Wang, X. Wei, R. Zhang, Y. Tu, T. Xia, L. Peng, Distinct *Miscanthus* lignocellulose improves fungus secreting cellulases and xylanases for consistently enhanced biomass saccharification of diverse bioenergy crops, Renew. Energ. 174 (2021) 799–809.
[19] H. Peng, W. Zhao, J. Liu, P. Liu, H. Yu, J. Deng, Q. Yang, R. Zhang, Z. Hu, S. Liu, D. Sun, L. Peng, Y. Wang, Distinct cellulose nanofibrils generated for improved Pickering emulsions and lignocellulose-degradation enzyme secretion coupled with high bioethanol production in natural rice mutants, Green Chem. 24 (2022) 2975–2987.
[20] R. Zhang, Z. Hu, H. Peng, P. Liu, Y. Wang, J. Li, J. Lu, Y. Wang, T. Xia, L. Peng, High density cellulose nanofibrils assembly leads to upgraded enzymatic and chemical catalysis of fermentable sugars, cellulose nanocrystals and cellulases production by precisely engineering cellulose synthases complexes, Green Chem. 25 (2023) 1096–1106.
[21] M. Madadi, K. Zhao, Y. Wang, Y. Wang, S. Tang, T. Xia, N. Jin, Z. Xu, G. Li, Z. Qi, L. Peng, Z. Xiong, Modified lignocellulose and rich starch for complete saccharification to maximize bioethanol in distinct polyploidy potato straw, Carbohyd. Polym. 265 (2021) 118070.
[22] D.Z. Ivetic, R.P. Omorjan, T.R. Dordevic, M.G. Antov, The impact of ultrasound pretreatment on the enzymatic hydrolysis of cellulose from sugar beet shreds: modeling of the experimental results, Environ. Prog. Sustain. 36 (2017) 1164–1172.
[23] L. Khedmat, A. Izadi, V. Mofid, S.Y. Mojtahedi, Recent advances in extracting pectin by single and combined ultrasound techniques: a review of technofunctional and bioactive health-promoting aspects, Carbohyd. Polym. 229 (2020) 115474.
[24] M.W. Easson, B. Condon, B.S. Dien, L. Iten, R. Slopek, M. Yoshioka-Tarver, A. Lambert, J. Smith, The application of ultrasound in the enzymatic hydrolysis of switch grass, Appl. Biochem. Biotechnol. 165 (2011) 1322–1331.
[25] Y. Li, P. Liu, J. Huang, R. Zhang, Z. Hu, S. Feng, Y. Wang, L. Wang, T. Xia, L. Peng, Mild chemical pretreatments are sufficient for bioethanol production in transgenic rice straws overproducing glucosidase, Green Chem. 20 (2018) 2047–2056.
[26] Z. Hu, Q. Li, Y. Chen, T. Li, Y. Wang, R. Zhang, H. Peng, H. Wang, Y. Wang, J. Tang, M. Aftab, L. Peng, Intermittent ultrasound retains cellulases unlock for enhanced cellulosic ethanol with high-porosity biochar for dye adsorption using desirable rice mutant straw, Bioresour. Technol. 369 (2023) 128437.
[27] Y. Wang, J. Huang, Y. Li, K. Xiong, Y. Wang, F. Li, M. Liu, Z. Wu, Y. Tu, L. Peng, Ammonium oxalate-extractable uronic acids positively affect biomass enzymatic digestibility by reducing lignocellulose crystallinity in *Miscanthus*, Bioresour. Technol. 196 (2015) 391–398.
[28] L. Cheng, L. Wang, L. Wei, Y. Wu, A. Alam, C. Xu, Y. Wang, Y. Tu, L. Peng, Combined mild chemical pretreatments for complete cadmium release and cellulosic ethanol co-production distinctive in wheat mutant straw, Green Chem. 21 (2019) 3693.
[29] T.K. Ghose, Measurement of cellulase activities, Pure Appl. Chem. 59 (1987) 257–268.
[30] M.M. Bradford, A rapid and sensitive method for the quantitation of microgram quantities of protein utilizing the principle of protein-dye binding, Anal. Biochem. 72 (1976) 248–254.
[31] J. Liu, X. Zhang, H. Peng, T. Li, P. Liu, H. Gao, Y. Wang, J. Tang, Q. Li, Z. Qi, L. Peng, T. Xia, Full-chain $FeCl_3$ catalyzation is sufficient to boost cellulase secretion and cellulosic ethanol along with valorized supercapacitor and biosorbent using desirable corn stalk, Molecules 28 (2023) 2060.
[32] C. Xu, M.A. Alam, Z. Wang, Y. Peng, C. Xie, W. Gong, Q. Yang, S. Huang, W. Zhuang, J. Xu, Co-fermentation of succinic acid and ethanol from sugarcane bagasse based on full hexose and pentose utilization and carbon dioxide reduction, Bioresour. Technol. 339 (2021) 125578.
[33] Z. Li, C. Zhao, Y. Zha, C. Wan, S. Si, F. Liu, R. Zhang, F. Li, B. Yu, Z. Yi, N. Xu, L. Peng, Q. Li, The minor wall-networks between monolignols and interlinked-phenolics predominantly affect biomass enzymatic digestibility in *Miscanthus*, PLoS One 9 (2014) e105115.
[34] C. Xu, T. Xia, H. Peng, P. Liu, Y. Wang, Y. Wang, H. Kang, J. Tang, M. Aftab, L. Peng, BsEXLX of engineered *Trichoderma reesei* strain as dual-active expansin to boost cellulases secretion for synergistic enhancement of biomass enzymatic saccharification in corn and *Miscanthus* straws, Bioresour. Technol. 376 (2023) 128844.
[35] L. Melton, Fungal architecture is a thing, and it's eye-catching, Nat. Biotechnol. 41 (2023) 1037.
[36] R.K. Sukumaran, M. Christopher, P.K. Valappil, A.S. Raju, R.M. Mathew, M. Sankar, A. Puthiyamadam, V.P. Adarsh, A. Awasthi, V. Rebinro, A. Abraham, A. Pandey, Addressing challenges in production of cellulases for biomass hydrolysis: targeted interventions into the genetics of cellulase producing fungi, Bioresour. Technol. 329 (2021) 124746.
[37] G.D. Saratale, R.G. Saratale, S. Varjani, S.K. Cho, G.S. Ghodake, A. Kadam, S. I. Mulla, R.N. Bharagava, D.S. Kim, S.S. Han, Development of ultrasound aided chemical pretreatment methods to enrich saccharification of wheat waste biomass for polyhydroxybutyrate production and its characterization, Ind. Crop Prod. 150 (2020) 112425.
[38] K.K. Puss, P. Paaver, M. Loog, S. Salmar, Ultrasound effect on a biorefinery lignin-cellulose mixture, Ultrason. Sonochem. 111 (2024) 107071.
[39] Z. Xiong, Y. Qin, J. Ma, L. Yang, Z. Wu, T. Wang, W. Wang, C. Wang, Pretreatment of rice straw by ultrasound-assisted Fenton process, Bioresour. Technol. 227 (2017) 408–411.
[40] Priya, P.R. Gogate, Ultrasound-assisted intensification of activity of free and immobilized enzymes: a review, Ind. Eng. Chem. Res. 60 (2021) 9650–9668.
[41] P.B. Subhedar, P.R. Gogate, Enhancing the activity of cellulase enzyme using ultrasonic irradiations, J. Mol. Catal. B-Enzym. 101 (2014) 108–114.
[42] C. Zhao, X. Liu, T. Zhan, J. He, Production of cellulase by *Trichoderma reesei* from pretreated straw and furfural residues, RSC Adv. 8 (2018) 36233.
[43] C. Li, D. Li, J. Feng, X. Fan, S. Chen, D. Zhang, R. He, Duckweed (Lemna minor) is a novel natural inducer of cellulase production in *Trichoderma reesei*, J. Biosci. Bioeng. 4 (2019) 486–491.
[44] L. Chen, G. Zou, J. Wang, J. Wang, R. Liu, Y. Jiang, G. Zhao, Z. Zhou, Characterization of the Ca^{2+}-responsive signaling pathway in regulating the expression and secretion of cellulases in *Trichoderma reesei* Rut-C30, Mol. Microbiol. 100 (2016) 560–575.
[45] H.C. Ong, W.H. Chen, Y. Singh, Y.Y. Gan, C.Y. Chen, P.L. Show, A state-of-the-art review on thermochemical conversion of biomass for biofuel production: a TG-FTIR approach, Energ. Convers. Manage. 209 (2020) 112634.
[46] Z. Cai, B. Ji, K. Yan, Q. Zhu, Investigation on reaction sequence and group site of citric acid with cellulose characterized by FTIR in combination with two-dimensional correlation spectroscopy, Polymer 11 (2019) 2071.
[47] H. Guo, C. Hong, X. Chen, Y. Xu, Y. Liu, D. Jiang, B. Zheng, Different growth and physiological responses to cadmium of the three *Miscanthus* species, PLoS One 11 (2016) 0153475.
[48] M. Balat, Production of bioethanol from lignocellulosic materials via the biochemical pathway: a review, Energy Convers. Manage. 52 (2011) 858–875.
[49] C. Xu, S. Hu, J. Xiang, L. Zhang, L. Sun, C. Shuai, Q. Chen, L. He, E.M. Edreis, Interaction and kinetic analysis for coal and biomass cogasification by TG-FTIR, Bioresour. Technol. 154 (2014) 313–321.
[50] A. Baum, M. Dominiak, S. Vidal-Melgosa, W.G. Willats, K.M. Sondergaard, P. W. Hansen, A.S. Meyer, J.D. Mikkelsen, Prediction of pectin yield and quality by FTIR and carbohydrate microarray analysis, Food Bioprocess Tech. 10 (2017) 143–154.
[51] H. Li, M. Xu, X. Yao, Y. Wen, S. Lu, J. Wang, B. Sun, The promoted hydrolysis effect of cellulase with ultrasound treatment is reflected on the sonicated rather than native brown rice, Ultrason. Sonochem. 83 (2022) 105920.
[52] X. Li, S. Mettu, G.J.O. Martin, M. Ashokkumar, C.S.K. Lin, Ultrasonic pretreatment of food waste to accelerate enzymatic hydrolysis for glucose production, Ultrason. Sonochem. 53 (2019) 77–82.
[53] H. Wang, S. Li, L. Wu, W. Zou, M. Zhang, Y. Wang, Z. Lv, P. Chen, P. Liu, Y. Yang, L. Peng, Y. Wang, Semi-overexpressed *OsMYB86L2* specifically enhances cellulose biosynthesis to maximize bioethanol productivity by cascading lignocellulose depolymerization via integrated rapid-physical and recyclable-chemical processes, Green Chem. 27 (2025) 9127.
[54] H. Zhang, Y. Wang, H. Peng, B. He, Y. Li, H. Wang, Z. Hu, H. Yu, Y. Wang, M. Zhou, L. Peng, M. Wang, Distinct lignocelluloses of plant evolution are optimally selective for complete biomass saccharification and upgrading Cd^{2+}/Pb^{2+} and dye adsorption via desired biosorbent assembly, Bioresour. Technol. 417 (2024) 131856.
[55] H. Yu, G. Zhang, J. Liu, P. Liu, H. Peng, Z. Teng, Y. Li, X. Ren, C. Fu, J. Tang, M. Li, Y. Wang, L. Wang, L. Peng, A functional cascading of lignin modification via repression of caffeic acid O-methyltransferase for bioproduction and anti-oxidation in rice, J. Adv. Res. 78 (2025) 1–9.
[56] J. Li, Y. Wang, Y. Zhou, S. Tan, J. Liu, Q. Zhang, R. Yang, H. Peng, P. Liu, Y. Wang, L. Peng, H. Kang, Integrative mechanisms of Mn peroxidase-dominated fungal digestion and CaO depolymerization for synergistic enhancement of biomass saccharification towards distinct bioethanol and lactic acid conversions in desired *Miscanthus*, Ind. Crop Prod. 246 (2026) 123224.
[57] R. Zhang, Z. Hu, Y. Wang, H. Hu, F. Li, M. Li, A. Ragauskas, T. Xia, H. Han, J. Tang, H. Yu, B. Xu, L. Peng, Single-molecular insights into the breakpoint of cellulose nanofibers assembly during saccharification, Nat. Commun. 14 (2023) 1100.
[58] S. Lu, L. Sun, Y. Wang, H. Peng, B. He, X. Yuan, Y. Wang, T. Xia, L. Peng, P. Liu, Dual-upgraded biomass saccharification and bioethanol production by cascading peptides interactions with polymers and activating cellulases in bioenergy crops, Renew. Energ. 256 (2026) 124651.